
CROSS-VIEW OPEN-VOCABULARY OBJECT DETECTION IN AERIAL IMAGERY

Jyoti Kini Rohit Gupta Mubarak Shah

Center for Research in Computer Vision, University of Central Florida, Orlando, Florida
 {jyoti.kini, rohit.gupta}@ucf.edu, shah@crcv.ucf.edu

ABSTRACT

Traditional object detection models are typically trained on a fixed set of classes, limiting their flexibility and making it costly to incorporate new categories. Open-vocabulary object detection addresses this limitation by enabling models to identify unseen classes without explicit training. Leveraging pretrained models contrastively trained on abundantly available ground-view image-text classification pairs provides a strong foundation for open-vocabulary object detection in aerial imagery. Domain shifts, viewpoint variations, and extreme scale differences make direct knowledge transfer across domains ineffective, requiring specialized adaptation strategies. In this paper, we propose a novel framework for adapting open-vocabulary representations from ground-view images to solve object detection in aerial imagery through structured domain alignment. The method introduces contrastive image-to-image alignment to enhance the similarity between aerial and ground-view embeddings and employs multi-instance vocabulary associations to align aerial images with text embeddings. Extensive experiments on the xView, DOTAv2, VisDrone, DIOR, and HRRSD datasets are used to validate our approach. Our open-vocabulary model achieves improvements of +6.32 mAP on DOTAv2, +4.16 mAP on VisDrone (Images), and +3.46 mAP on HRRSD in the zero-shot setting when compared to finetuned closed-vocabulary dataset-specific model performance, thus paving the way for more flexible and scalable object detection systems in aerial applications.

1 INTRODUCTION

Over the last decade, object detection has seen remarkable progress, with models attaining high accuracy on predefined categories in closed-set settings He et al. (2017); Ren et al. (2015); Carion et al. (2020). However, real-world applications demand open-vocabulary object detection, where models must recognize and localize unseen object categories. The emergence of large-scale pre-trained Vision-Language Models (VLMs) Radford et al. (2021); Jia et al. (2021) has significantly advanced open-vocabulary object detection, enabling models to detect novel categories beyond their training set. Among these, contrastive vision-language models Ranasinghe et al. (2023); Khan & Fu (2023); Ak et al. (2024); Cui et al. (2022) such as OWLv2 Minderer et al. (2023) leverage large-scale image-text pairings to learn generalizable representations, facilitating zero-shot object detection and retrieval. While these models achieve strong performance in ground-view imagery, extending them to aerial-view object detection remains a fundamental challenge due to domain shifts and viewpoint variations. Aerial imagery introduces unique complexities: extreme scale variations, occlusions, and drastic perspective distortions, making direct transfer of ground-view models ineffective.

Researchers have developed ground-to-aerial domain adaptation techniques to leverage the abundance of labeled ground-level image data for aerial object detection. Existing approaches address the domain gap through generative modeling Zeng et al. (2024); Ma et al. (2024); Soto et al. (2020); Ye et al. (2024); Lu et al. (2020), adversarial training Chen et al. (2021); Wozniak et al. (2024), self-supervised learning Scheibenreif et al. (2024); Wang et al. (2024a), viewpoint-dependent feature matching Mule et al. (2025); Hou et al. (2023); Shan et al. (2014); Shugaev et al. (2024); Regmi & Shah (2019), and knowledge distillation Yao et al. (2024); Wang et al. (2024b).

Generative models, such as GANs, synthesize aerial-like images from ground-view data, expanding training datasets and enhancing model generalization. Adversarial domain adaptation reduces domain shift by training a discriminator to distinguish between ground and aerial feature distributions while guiding the model to learn domain-invariant representations. Self-supervised learning lever-

ages the structure of unlabeled aerial images through pretext tasks like rotation prediction, enabling the model to learn useful representations without explicit supervision. Viewpoint-dependent feature matching establishes correspondences between ground and aerial imagery by leveraging geometric relationships, ensuring better feature alignment. Lastly, knowledge distillation transfers information from a ground-view teacher model to a student model optimized for aerial detection, facilitating effective cross-domain knowledge transfer.

Beyond domain adaptation, research in open-vocabulary aerial detection aims to recognize objects outside the set of categories encountered during training. CastDet Li et al. (2024) utilizes a self-learning framework based on a student-teacher paradigm, integrating RemoteCLIP Liu et al. (2024a) to generate class-agnostic region proposals and pseudo-labels, thereby enabling open-vocabulary detection in aerial imagery. Another approach, SS-OWFormer Mullappilly et al. (2024), designed for satellite imagery, employs a feature-alignment mechanism alongside pseudo-labeling to enhance the detection of previously unseen objects. However, these methods heavily depend on large-scale aerial datasets for finetuning, pseudo-labeling, or feature alignment, making them reliant on labeled aerial supervision. In practice, such large-scale labeled datasets are often scarce or unavailable in the aerial domain, which further limits the applicability of these approaches.

In contrast, we propose a novel approach leveraging the abundance of ground-view image-text data available and align it with aerial representations using a contrastive learning framework, as seen in Fig. 1. Unlike approaches that require dataset-specific finetuning, which can lead to catastrophic forgetting of ground-view knowledge (refer Fig. 2), our contrastive learning formulation preserves pretrained vision-language model knowledge while ensuring robust cross-view feature alignment. Our vocabulary expansion enhances zero-shot detection of novel objects, making it more scalable and adaptable for open-vocabulary aerial object detection compared to existing approaches.

The key contributions of this work are as follows:

- a. Contrastive Image-to-Image Alignment:** We introduce a novel contrastive alignment strategy that enhances semantic consistency between aerial-view and ground-view embeddings, facilitating the transfer of meaningful features from ground-view pretrained vision-language models (VLMs) to open-vocabulary object detection in aerial imagery.
- b. Multi-Instance Vocabulary Association:** We propose a multi-instance vocabulary association technique that aligns aerial images with text embeddings, effectively leveraging textual descriptions to improve recognition of unseen categories in aerial view images.
- c. Extensive Benchmark Evaluation:** We validate experiments on the xView Lam et al. (2018), DOTAv2 Ding et al. (2021), VisDrone Cao et al. (2021), DIOR Li et al. (2020), and HRRSD Zhang et al. (2019) datasets, achieving significant improvements in open-vocabulary detection performance, highlighting the scalability and effectiveness of our method.

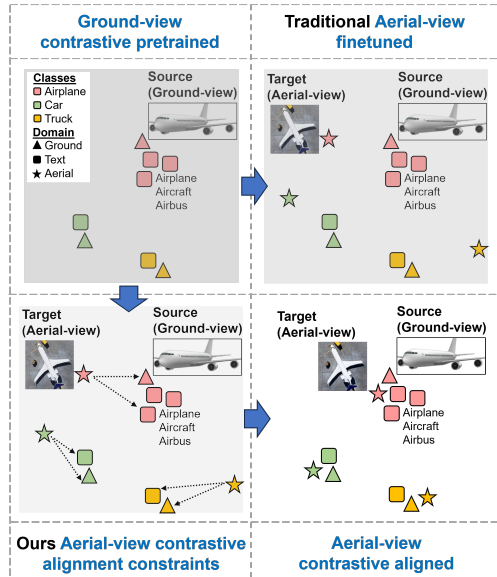


Figure 1: **Motivation:** Ground-view contrastive pretrained open vocabulary detectors (top-left) fail to generalize to aerial views, and traditional finetuning (top-right) results in misaligned feature spaces. Our method (bottom-left) enforces cross-view contrastive alignment and aerial view-text associations, ensuring better semantic consistency and generalization for open-vocabulary aerial object detection (bottom-right). *Note:* Different object classes are color-coded: **Airplane**, **Car**, **Truck**. Different domains are shape-coded: **▲** Ground-view, **■** Text, **★** Aerial-view.

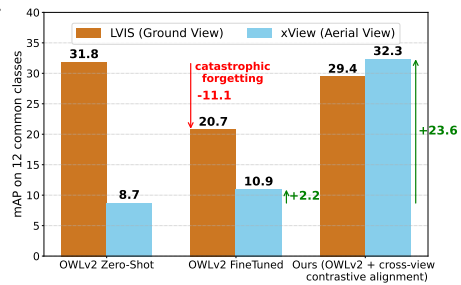


Figure 2: Our approach improves aerial-view detection while preserving ground-view performance and avoids catastrophic forgetting typical of naive finetuning.

2 RELATED WORK

Aerial Object Detection Deep learning has significantly advanced object detection in natural/ground-view images, leading to the adaptation of frameworks like Faster R-CNN Girshick (2015), RetinaNet Lin et al. (2017), YOLO Redmon et al. (2016), and DETR Zhu et al. (2020) for aerial imagery. However, aerial object detection faces challenges such as extreme scale variations, arbitrary orientations, and high object density. To address these challenges, methods like ROI-Transformer, R3Det Yang et al. (2021), and RSDet++ Qian et al. (2022) improve localization accuracy by using oriented bounding boxes, while techniques such as SCRDet Yang et al. (2019b) and ClusDet Yang et al. (2019a) enhance the detection of small and densely packed objects. Frameworks like Focus-and-Detect Koyun et al. (2022) and PARE-YOLO Zhang et al. (2025) further refine small object detection through clustering and multi-scale feature fusion. NavBLIP Li et al. (2025) integrates visual and contextual information for UAV-based detection, enhancing performance in dynamic environments. Despite these advancements, most methods operate under a closed-set assumption, meaning they are trained and evaluated on a fixed set of object categories. Expanding such models to recognize novel categories requires collecting large-scale annotated datasets, a costly and time-intensive process.

Open-Vocabulary Object Detection (OVD) Early work such as OVR-CNN Zareian et al. (2021) used bounding box annotations for a limited set of objects while leveraging image-caption pairs to extend the detection vocabulary. With the advent of pretrained Vision-Language Models (VLMs) like CLIP Radford et al. (2021) and ALIGN Jia et al. (2021), recent OVD approaches have transferred text-image knowledge into detection models using prompt learning and region-level finetuning. Methods like ViLD Gu et al. (2021) employ vision-language distillation to align textual and visual features, RegionCLIP Zhong et al. (2022) aligns region-level representations with textual concepts, and Detic Zhou et al. (2022) enhances detection capabilities by incorporating large-scale image classification datasets. Further refinements, including PromptDet Feng et al. (2022) and DetPro Du et al. (2022), optimize prompt embeddings for better visual-textual alignment. Additionally, models like YOLO-World Cheng et al. (2024) and F-VLM Kuo et al. (2022) address open-vocabulary detection challenges. YOLO-World integrates real-time vision-language modeling with Ultralytics YOLOv8, enabling efficient object detection based on descriptive text. F-VLM simplifies the training process by using frozen vision and language models, achieving state-of-the-art results with reduced computational overhead. Despite these advancements, applying OVD to aerial imagery remains challenging due to smaller dataset sizes and fundamental differences from ground-view images.

3 APPROACH

Recent advancements in vision-language models (VLMs) have significantly improved open-vocabulary object detection by aligning images and text in a shared embedding space. Our framework builds upon this idea to tackle cross-view open-vocabulary object detection, specifically aligning aerial-view images with ground-view and textual representations. Our model consists of a vision encoder f_θ and a text encoder h_ϕ , which respectively project aerial images and textual queries into a common feature space. Given an aerial image I_A , the vision encoder extracts its feature representation $f_\theta(I_A) \in \mathbb{R}^d$, where d is the size of the embedding space. Similarly, a textual query Y is tokenized and processed by the text encoder h_ϕ , producing a textual feature embedding $h_\phi(Y) \in \mathbb{R}^d$.

To ensure effective alignment between aerial, ground, and textual representations, our model incorporates two key learning mechanisms: Cross-View Representation Alignment (Sec. 3.1) and Aerial-Text Multi-Instance Association (Sec. 3.2). The success of these alignment strategies depends on the quality of the generated contrastive alignment data. To construct this, we introduce a data generation pipeline comprising Aerial-Ground Object Detection Correspondence (Sec. 3.3) and Aerial-Text Vocabulary Expansion (Sec. 3.4).

3.1 CROSS-VIEW REPRESENTATION ALIGNMENT

Standard contrastive vision-language models struggle to generalize from ground-view pretraining to aerial views due to the modality gap introduced by viewpoint shifts and domain discrepancies. Instead of direct finetuning on aerial imagery, we propose a cross-view contrastive alignment strategy that explicitly bridges the feature spaces of aerial and ground representations.

Given a batch of aerial images I_A and corresponding ground-view references I_G , we apply contrastive learning to enforce similarity between aerial-ground pairs, while simultaneously pushing

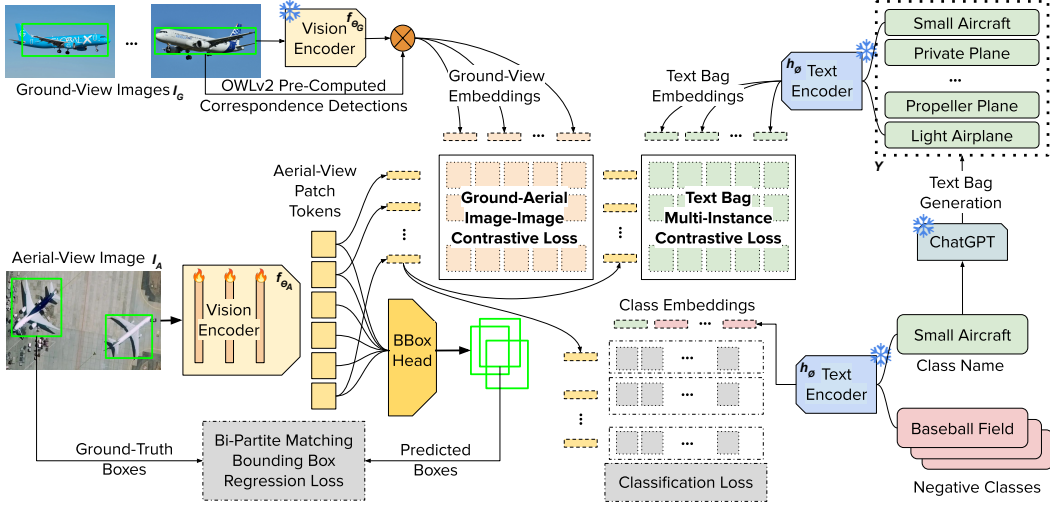


Figure 3: **Overview** Traditional open-vocabulary object detector finetuning includes two losses: a bi-partite matching based bounding box regression loss and a classification loss computed in the shared image–text embedding space. We further introduce two new components: a **ground–aerial contrastive loss** that aligns aerial and ground image embeddings, and a **text-bag multi-instance contrastive loss** that aligns aerial features with text bags. To realize these objectives, we generate an aerial–ground correspondence dataset providing cross-view positives/negatives, and also expand the class vocabulary by using ChatGPT to synthesize variants of class names (“text bags”) consumed by the text encoder. Joint optimization over these losses places aerial \leftrightarrow ground \leftrightarrow text representations in a cohesive shared embedding space, yielding stronger zero-shot generalization in aerial imagery.

apart non-matching samples. Since only the aerial-view encoder is finetuned during training, we use a single notation f_{θ} to refer to the model being optimized, simplifying the formulation:

$$\mathcal{L}_{Image_A-Image_G} = -\frac{1}{N} \sum_{i=1}^N \log \frac{\exp(f_{\theta}(I_A^i)^{\top}, f_{\theta}(I_G^i))/\rho}{\sum_{j=1}^N \exp(f_{\theta}(I_A^i)^{\top}, f_{\theta}(I_G^j))/\rho}, \quad (1)$$

where N represents the batch size, i indexes a positive (correctly matched) aerial-ground pair, and j indexes all samples in the batch. The numerator maximizes the similarity between the correct aerial-ground pair (I_A^i, I_G^i) , while the denominator contrasts it against all ground-view images I_G^j in the batch, encouraging better separation between matching and non-matching samples. Here, ρ is a temperature parameter controlling the sharpness of the similarity distribution.

By omitting a subscript for f_{θ} , we emphasize that only one encoder is being finetuned (i.e., the aerial-view encoder), while the ground-view embeddings remain fixed, ensuring efficient adaptation of aerial representations to the pretrained feature space.

3.2 AERIAL-TEXT MULTI-INSTANCE ASSOCIATION

To further improve generalization, we introduce multi-instance contrastive learning between aerial images and their corresponding textual descriptions. Rather than enforcing a strict one-to-one correspondence, we adopt a multi-instance text association approach, where each aerial image I_A^i is linked to a set of semantically related textual queries via a text-bag representation. This formulation enables better alignment between aerial imagery and natural language descriptions by accounting for ambiguities and variations in object naming conventions.

Our objective function extends MIL-NCE Miech et al. (2020), optimizing the alignment between aerial images and a diverse set of textual candidates:

$$\mathcal{L}_{Image_A-Text} = -\frac{1}{N} \sum_{i=1}^N \log \frac{\sum_k \sum_n \exp(h_{\phi}(Y_{k,n})^{\top} f_{\theta}(I_A^i)/\sigma)}{\sum_j \sum_n \exp(h_{\phi}(Y_{j,n})^{\top} f_{\theta}(I_A^i)/\sigma)}, \quad (2)$$

where N represents the batch size, index i refers to an aerial image I_A^i , while j iterates over all possible textual descriptions in the batch. The index k corresponds to a positive text-bag group,

which contains multiple semantically related textual descriptions for I_A^i , and n indexes the individual text descriptions within the text-bag. The numerator sums over multiple positive textual descriptions $Y_{k,n}$ associated with I_A^i , while the denominator contrasts it against all text samples $Y_{j,n}$ in the batch, ensuring that the model learns to distinguish between relevant and irrelevant textual associations. This multi-instance contrastive loss promotes robust open-vocabulary object detection.

3.3 AERIAL-GROUND OBJECT DETECTION CORRESPONDENCE

In cross-view object detection, establishing category-based correspondence between aerial and ground-view detections is crucial for model generalization. Our data generation pipeline constructs aerial-ground correspondences by leveraging existing datasets (namely xView Lam et al. (2018) for aerial and LVIS Gupta et al. (2019) / CC12M Changpinyo et al. (2021) for ground) and enhancing them with inferred-labeling techniques. The goal is to align aerial detections with semantically corresponding ground-view samples while ensuring sufficient diversity. To facilitate cross-view representation learning for open-vocabulary aerial object detection, we construct a dataset $D_{aligned}$ by establishing correspondences between aerial and ground-view images. This process consists of two primary

steps: **Direct Correspondence**, as shown in Fig. 4, where detection matches between aerial and ground images are identified based on category, and **Inferred Correspondence**, where pseudo-matches are generated for categories that lack ground-view annotations. The final step involves **Augmentation and Normalization** to enhance the generated data’s diversity and consistency.

Direct Correspondence (For Common Categories): For object categories present in both the aerial and ground datasets, we directly extract aligned object instances. As seen in Algo. 1, for each category c in the set of common categories C_{common} , we retrieve bounding box annotations B_G and corresponding images I_G from the ground-view dataset. These ground-view instances are then paired with their aerial counterparts, forming structured dataset entries (B_A, B_G, y_c) , where B_A represents the aerial bounding box, B_G is the corresponding ground bounding box, and y_c is the class label. This process ensures precise alignment between aerial and ground perspectives, establishing a strong foundation for shared representations.

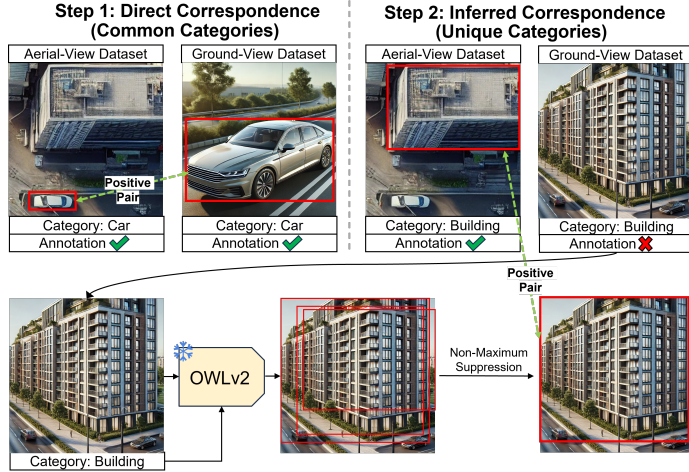


Figure 4: **Aerial-Ground Object Detection Correspondence** Step 1 (top-left) shows a case where the category ‘Car’ is annotated in both aerial and ground-view datasets, allowing direct positive pair generation using ground-truth annotations. Step 2 (top-right) illustrates a case where the category ‘Building’ lacks ground-view annotations. To address this, OWLv2 is used to generate detections in the ground-view image (bottom row), followed by non-maximum suppression to establish cross-view correspondence data for our contrastive alignment training.

Algorithm 1: Aerial-Ground Object Detection Correspondence

```

1: Initialize:  $D_{aligned} \leftarrow \emptyset$  # Empty dataset
    $\triangleright$  Step 1: Direct Correspondence (Common Categories)
2: for  $c \in C_{common}$  do
3:   Extract  $\{B_G, I_G\}$  # Ground Boxes, Images
4:    $D_{aligned} \leftarrow D_{aligned} \cup \{(B_A, B_G, y_c)\}$ 
5: end for
    $\triangleright$  Step 2: Inferred Correspondence (Unique Categories)
6: for  $c \in C_{unique}$  do
7:    $\hat{B}_G \leftarrow \text{OWLv2}(I_G)$  # Generate ground boxes
8:    $\hat{B}_G \leftarrow \text{NMS}(\hat{B}_G, \tau)$  # Remove redundant
9:    $D_{aligned} \leftarrow D_{aligned} \cup \{(B_A, \hat{B}_G, y_c)\}$ 
10: end for
    $\triangleright$  Step 3: Augmentation & Normalization
11:  $D_{aligned} \leftarrow \text{Augment}(D_{aligned})$  # Crop, Rotate
12:  $D_{aligned} \leftarrow \text{Norm}(D_{aligned})$  # Feature Align
13: Return  $D_{aligned}$  # Store for training

```

Inferred Correspondence (For Unique Categories): For categories that exist in the aerial dataset but lack explicit ground-view annotations, we generate inferred correspondences using vision-language models. For each category $c \in C_{unique}$, we apply OWLv2 to detect objects in the ground-view dataset, producing an initial set of bounding boxes \hat{B}_G . To refine these detections, we employ Non-Maximum Suppression (NMS) with a confidence threshold τ to eliminate redundant or low-confidence detections, ensuring only reliable bounding boxes are retained. The final pseudo-ground view detections \hat{B}_G are then associated with aerial objects, forming dataset pairs (B_A, \hat{B}_G, y_c) . This inferred alignment enables training on categories that lack explicit ground-truth annotations.

Augmentation and Normalization: To enhance dataset robustness and improve alignment consistency, we apply a series of augmentation and normalization techniques. Geometric transformations, such as cropping and rotation, diversify the dataset and mitigate overfitting. Additionally, feature normalization is applied to harmonize aerial and ground embedding spaces, ensuring better compatibility during model training. After these refinements, the final dataset $D_{aligned}$ is stored for training.

3.4 AERIAL-TEXT VOCABULARY EXPANSION

Here, we focus on enhancing category representation by expanding textual variations of aerial object categories. The primary goal is to improve the model’s ability to recognize multiple textual references for the same object, enabling effective aerial object detection in open-vocabulary scenarios. The process begins by initializing an empty dataset D_{text} to store textual variations of aerial object categories. As seen in Algo. 2, for each category c in the aerial dataset C_A , ChatGPT is utilized to generate a set of label variations \mathcal{V}_c .

These variations include synonymous terms, alternative phrasings, and domain-specific terminology that may be used to refer to the same object in different contexts. The generated variations are stored in D_{text} as pairs of the original category c and its corresponding set of variations \mathcal{V}_c . Once all categories are processed, the dataset D_{text} is finalized and returned for use in training. This expansion follows a hierarchical association where each category serves as a parent node with multiple semantically related variations acting as child nodes. By structuring the data in this way, the model can better interpret and generalize aerial object classes in an open-vocabulary setting.

It is worth noting that while our data generation pipeline (Aerial-Ground Object Detection Correspondence and Aerial-Text Vocabulary Expansion) provides essential correspondences and variations, the key novelty lies in how these resources are exploited through structured contrastive alignment, rather than in dataset construction itself.

4 EXPERIMENTS

We evaluate zero-shot transfer on unseen aerial benchmarks and compare our approach with state-of-the-art open-vocabulary detectors. We also carry out ablation studies to evaluate the impact of various design decisions, such as encoder patch size, loss contributions etc.

Training Data. Our pipeline builds cross-view correspondences and expands the vocabulary to strengthen contrastive alignment. Between xView and LVIS, 12 categories overlap and 48 are unique to xView. We create 25,403 positive aerial \leftrightarrow ground pairs via direct matches, rising to 50,650 with inferred correspondences; adding CC12M brings the total to 310,548 pairs. Vocabulary expansion grows 60 aerial categories into 360 variants, broadening textual coverage (examples in Tab. 1).

Algorithm 2: Vocabulary Expansion

```

1: Initialize:  $D_{text} \leftarrow \emptyset$  # Empty dataset
2: for  $c \in C_A$  do
3:    $\mathcal{V}_c \leftarrow \text{ChatGPT}(c)$  # Generate label variations
4:    $D_{text} \leftarrow D_{text} \cup \{(c, \mathcal{V}_c)\}$ 
5: end for
6: Return  $D_{text}$  # Store for training

```

Category	Variations
Small Aircraft	Light airplane, Private plane, Single-engine aircraft, Propeller plane, Cessna-type aircraft, General aviation aircraft
Helicopter	Chopper, Rotary-wing aircraft, Rotorcraft, Helo, Air ambulance, Military helicopter, Rescue helicopter
Shed	Storage shed, Outbuilding, Toolshed, Garden shed, Small barn
Excavator	Digger, Backhoe, Trackhoe, Mechanical shovel, Hydraulic excavator
Small Car	Compact car, Hatchback, Subcompact vehicle, Economy car, City car, Two-door car, Four-door car

Table 1: Vocabulary expansion examples.

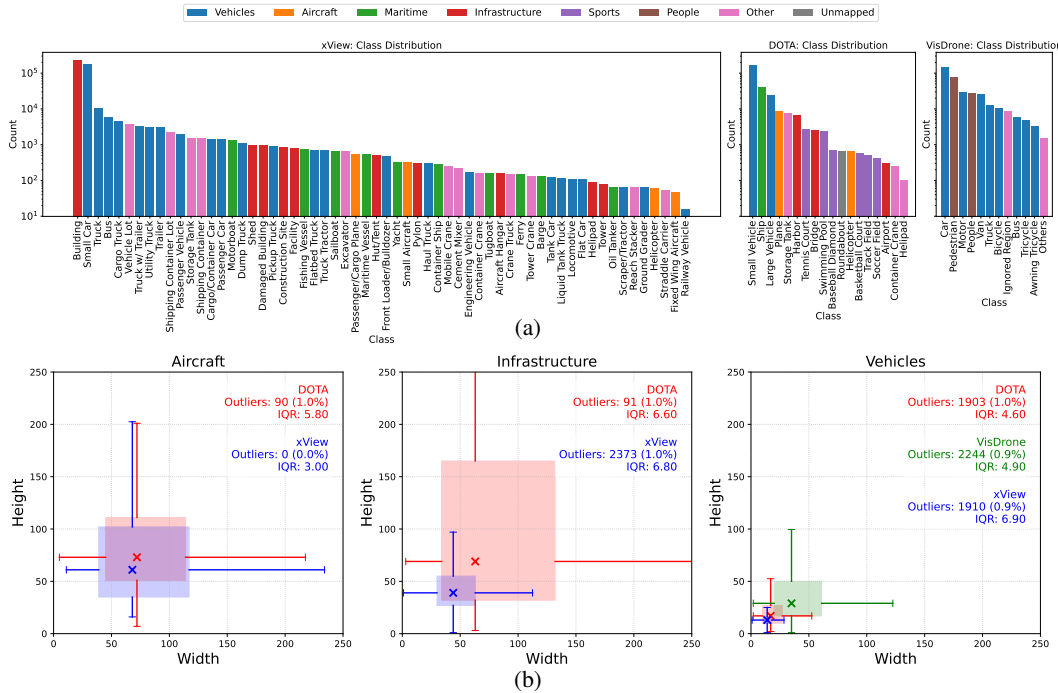


Figure 5: **Distribution** of (a) object categories and (b) size variations across three remote sensing datasets: xView, DOTA2, and VisDrone (Images). The figure highlights category imbalance and significant object scale variations, reflecting challenges in open-vocabulary aerial object detection.

Evaluation Datasets. We evaluate generalization on five remote-sensing benchmarks: xView Lam et al. (2018), DOTA2 Ding et al. (2021), VisDrone (images/videos) Cao et al. (2021), DIOR Li et al. (2020), and HRRSD Zhang et al. (2019). These datasets span satellite, aerial, and drone imagery. Collectively, they contain millions of labeled objects across dozens of categories with wide variation in scale, orientation, and scene complexity, stressing robustness to different sensors, viewpoints, conditions, and object sizes. Fig. 5 summarizes instance and size distributions, revealing pronounced category imbalance and scale variation, which are key challenges for open-vocabulary aerial object detection.

Metrics For our evaluation, we utilize the standard $AP_{50:95}$ metric, adhering to the benchmarking protocol set by MS COCO Lin et al. (2014). Further to assess overall performance across both seen and unseen object classes we utilize Harmonic Mean (HM) of mAP_{base} and mAP_{novel} classes.

4.1 ZERO-SHOT GENERALIZATION IN AERIAL DATASETS

Our model is trained only on our generated xView-LVIS cross-view vocabulary-expanded data and evaluated in a zero-shot manner on DOTA2, VisDrone, DIOR, and HRRSD, with *no* training data from those test datasets. In all experiments, we consistently refer to this protocol as *zero-shot transferability*. In Tab. 2, we compare our zero-shot object detection approach against YOLOv11 (finetuned) Jocher & Qiu (2024), which is trained on the entire dataset, across six aerial datasets: xView, DOTA2, VisDrone (Images), VisDrone (Videos), DIOR, and HRRSD. In contrast, our model never sees these datasets during training, yet achieves consistent improvements in a zero-shot setting, with performance gains of **+6.32** on DOTA2, **+4.16** on VisDrone (Images), **+2.37** on VisDrone (Videos), **+2.23** on DIOR, and **+3.46**

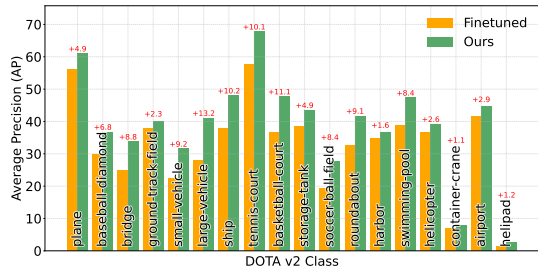


Figure 6: Per-class zero-shot performance of our model on DOTA2 outperforms finetuning.

on HRRSD over YOLO. For xView, which is not evaluated in a true zero-shot setting (*), our approach still improves by **+2.99**. These results highlight our model’s strong cross-domain generalization, demonstrating competitive performance without dataset-specific finetuning. Refer to Fig. 7 for qualitative results across datasets and Fig. 6 for the per-class breakdown on DOTAv2.

Datasets	Finetuned		Zero-Shot
	OWLv2	YOLOv11	Ours
xView Lam et al. (2018)	12.65	34.92	37.91* (+2.99)
DOTAv2 Ding et al. (2021)	15.01	32.28	38.60 (+6.32)
VisDrone (Images) Cao et al. (2021)	25.70	40.81	44.97 (+4.16)
VisDrone (Videos) Cao et al. (2021)	18.44	34.65	37.02 (+2.37)
DIOR Li et al. (2020)	45.91	61.68	63.91 (+2.23)
HRRSD Zhang et al. (2019)	53.25	70.66	74.12 (+3.46)

Table 2: Comparison of OWLv2 (Finetuned), YOLO (Finetuned) and our zero-shot approach across multiple datasets. Note: “*” xView is not evaluated in a zero-shot setting.



Figure 7: Qualitative results across diverse aerial dataset scenarios, including maritime environments (1, 2), sports facilities (3), nighttime conditions (4, 5), urban scenes featuring multiple interacting object classes (6, 7, 8), and pedestrians across widely varying viewpoints (9, 10).

Method	External	\mathcal{T}_{novel}	\mathcal{T}_{cls}	mAP	mAP _{base}	mAP _{novel}	HM
Detic	NWPU-RESISC45	✗	✓	16.8	19.8	4.8	7.7
ViLD	DIOR	✓	✗	25.6	28.5	14.2	19.0
OV-DETR	DIOR	✓	✗	25.6	25.6	25.5	25.6
BARON	NWPU-RESISC45	✗	✓	27.4	29.4	19.5	23.5
YOLO-World	NWPU-RESISC45	✗	✓	32.9	39.1	8.5	13.9
GroundingDINO	NWPU-RESISC45	✗	✓	33.0	40.5	3.3	6.1
GLIP	NWPU-RESISC45	✗	✓	33.8	41.0	5.4	9.5
CastDet	DIOR	✗	✗	38.5	36.5	46.5	40.9
CastDet	DIOR	✓	✗	40.5	39.0	46.3	42.3
<i>Ours</i>	xView	✗	✗	44.9	42.7	49.2	45.7

Table 3: Performance comparison of SOTA open-vocabulary object detection methods on the VisDrone (Images) dataset. Here, \mathcal{T}_{novel} indicates whether novel classes are pre-known, while \mathcal{T}_{cls} denotes whether additional classification or caption datasets are used during training. The best method is shown in **Red**, and the second-best method is shown in **Blue**.

4.2 COMPARISON TO STATE-OF-THE-ART

As seen in Tab. 3, our method surpasses existing state-of-the-art open-vocabulary object detection approaches on the VisDrone (Images) dataset. These gains underscore the effectiveness of our aerial-ground alignment and aerial-text association.

4.3 ABLATION STUDIES

4.3.1 VISION ENCODER PATCH SIZE

The ablation study in Tab. 4 assesses the impact of vision encoder patch size (Patch-16 vs. Patch-14) on open-vocabulary aerial object detection. Smaller patch sizes (Patch-14) consistently improve performance across all datasets, with DOTAv2 showing the largest gain of **+4.63**. This improvement is likely due to Patch-14 capturing finer spatial details, leading to better feature granularity and enhanced object discrimination, especially in high-variance aerial imagery.

Datasets	Patch Size	
	<i>Ours (/16)</i>	<i>Ours (/14)</i>
xView	36.48*	37.91* (+1.43)
DOTAv2	33.97	38.60 (+4.63)
VisDrone (Images)	42.66	44.97 (+2.31)
VisDrone (Videos)	35.78	37.02 (+1.24)

Table 4: Impact of encoder patch size on open-vocabulary aerial detection performance. Note: ‘*’ indicates xView is not evaluated zero-shot.

4.3.2 AERIAL-GROUND CORRESPONDENCE DATASET

Tab. 5 compares detection performance on xView and DOTAv2 when using different aerial-ground correspondence datasets (LVIS vs. CC12M) for alignment. CC12M leads to a substantial performance improvement across both datasets (**+3.23** on xView, **+6.87** on DOTAv2), highlighting the benefits of a larger and more diverse dataset for cross-view feature alignment. Aerial-ground alignment benefits from larger and more diverse datasets, as seen with CC12M outperforming LVIS. This suggests that training with a broader distribution of images improves cross-view generalization and enhances feature transferability, particularly for open-vocabulary aerial detection. The effect is more pronounced on DOTAv2, due to its higher scene complexity, where additional aerial-ground associations provide stronger supervision.

Evaluation Dataset	Aerial-Ground Correspondences	
	<i>LVIS</i>	<i>CC12M</i>
xView	33.25	36.48
DOTAv2	27.10	33.97

Table 5: Performance comparison on xView and DOTAv2 using different datasets (LVIS, CC12M) as the source of aerial-ground correspondence.

4.3.3 CONTRIBUTION OF CONTRASTIVE LOSSES

The individual contributions of $Image_A-Text$ and $Image_A-Image_G$ contrastive losses to overall cumulative performance on the xView and DOTAv2 datasets are evaluated in Tab. 6. The $Image_A-Text$ contrastive loss aligns aerial image features with textual representations, facilitating open-vocabulary recognition, whereas the $Image_A-Image_G$ contrastive loss enforces aerial-to-ground view consistency, improving domain adaptation. The cumulative score reflects the combined effect of both losses, highlighting that $Image_A-Image_G$ contrastive learning plays a more dominant role in feature alignment, as indicated by its higher individual contribution. However, the synergy between both losses leads to the best overall performance, demonstrating the importance of multi-modal representation learning in cross-view object detection.

Datasets	Contrastive Losses		
	$Image_A-Text$	$Image_A-Image_G$	Both
xView	26.13	32.41	33.25
DOTAv2	19.98	25.06	27.10

Table 6: Impact of individual losses.

5 CONCLUSION

We propose a novel cross-view contrastive alignment framework for open-vocabulary object detection in aerial imagery. To facilitate this, we establish aerial-ground correspondences using xView, LVIS, and CC12M, generating a large corpus of correspondence pairs. To bridge the modality gap between aerial and ground views, we establish cross-view alignment by learning semantic correspondences between detected objects across perspectives. Furthermore, we enhance generalization by employing multi-instance contrastive learning to align aerial images with their textual descriptions. Through extensive experiments, we demonstrate that our approach in a zero-shot setting outperforms finetuned models, advancing the scalability and adaptability of aerial object detection.

Acknowledgment

This work was conducted at UCF and supported by Lockheed Martin Corporate Engineering.

REFERENCES

- Kenan Emir Ak, Jay Mohta, Dimitris Dimitriadis, Saurav Manchanda, Yan Xu, and Mingwei Shen. Aligning vision language models with contrastive learning. 2024.
- Yaru Cao, Zhijian He, Lujia Wang, Wenguan Wang, Yixuan Yuan, Dingwen Zhang, Jinglin Zhang, Pengfei Zhu, Luc Van Gool, Junwei Han, et al. Visdrone-det2021: The vision meets drone object detection challenge results. In *Proceedings of the IEEE/CVF International conference on computer vision*, pp. 2847–2854, 2021.
- Nicolas Carion, Francisco Massa, Gabriel Synnaeve, Nicolas Usunier, Alexander Kirillov, and Sergey Zagoruyko. End-to-end object detection with transformers. In *European conference on computer vision*, pp. 213–229. Springer, 2020.
- Soravit Changpinyo, Piyush Sharma, Nan Ding, and Radu Soricut. Conceptual 12m: Pushing web-scale image-text pre-training to recognize long-tail visual concepts. In *Proceedings of the IEEE/CVF conference on computer vision and pattern recognition*, pp. 3558–3568, 2021.
- Hua-Mei Chen, Andreas Savakis, Ashley Diehl, Erik Blasch, Sixiao Wei, and Genshe Chen. Targeted adversarial discriminative domain adaptation. *Journal of Applied Remote Sensing*, 15(3): 038504–038504, 2021.
- Tianheng Cheng, Lin Song, Yixiao Ge, Wenyu Liu, Xinggang Wang, and Ying Shan. Yolo-world: Real-time open-vocabulary object detection. In *Proceedings of the IEEE/CVF Conference on Computer Vision and Pattern Recognition*, pp. 16901–16911, 2024.
- Quan Cui, Boyan Zhou, Yu Guo, Weidong Yin, Hao Wu, Osamu Yoshie, and Yubo Chen. Contrastive vision-language pre-training with limited resources. In *European Conference on Computer Vision*, pp. 236–253. Springer, 2022.
- Jian Ding, Nan Xue, Gui-Song Xia, Xiang Bai, Wen Yang, Michael Ying Yang, Serge Belongie, Jiebo Luo, Mihai Datcu, Marcello Pelillo, et al. Object detection in aerial images: A large-scale benchmark and challenges. *IEEE transactions on pattern analysis and machine intelligence*, 44(11):7778–7796, 2021.
- Yu Du, Fangyun Wei, Zihe Zhang, Miaojing Shi, Yue Gao, and Guoqi Li. Learning to prompt for open-vocabulary object detection with vision-language model. In *Proceedings of the IEEE/CVF conference on computer vision and pattern recognition*, pp. 14084–14093, 2022.
- Chengjian Feng, Yujie Zhong, Zequn Jie, Xiangxiang Chu, Haibing Ren, Xiaolin Wei, Weidi Xie, and Lin Ma. Promptdet: Towards open-vocabulary detection using uncurated images. In *European conference on computer vision*, pp. 701–717. Springer, 2022.
- Ross Girshick. Fast r-cnn. In *Proceedings of the IEEE international conference on computer vision*, pp. 1440–1448, 2015.
- Xiuye Gu, Tsung-Yi Lin, Weicheng Kuo, and Yin Cui. Open-vocabulary object detection via vision and language knowledge distillation. *arXiv preprint arXiv:2104.13921*, 2021.
- Agrim Gupta, Piotr Dollar, and Ross Girshick. Lvis: A dataset for large vocabulary instance segmentation. In *Proceedings of the IEEE/CVF conference on computer vision and pattern recognition*, pp. 5356–5364, 2019.
- Kaiming He, Georgia Gkioxari, Piotr Dollár, and Ross Girshick. Mask r-cnn. In *Proceedings of the IEEE international conference on computer vision*, pp. 2961–2969, 2017.
- Qingfeng Hou, Jun Lu, Haitao Guo, Xiangyun Liu, Zhihui Gong, Kun Zhu, and Yifan Ping. Feature relation guided cross-view image based geo-localization. *Remote Sensing*, 15(20):5029, 2023.
- Chao Jia, Yinfei Yang, Ye Xia, Yi-Ting Chen, Zarana Parekh, Hieu Pham, Quoc Le, Yun-Hsuan Sung, Zhen Li, and Tom Duerig. Scaling up visual and vision-language representation learning with noisy text supervision. In *International conference on machine learning*, pp. 4904–4916. PMLR, 2021.

-
- Glenn Jocher and Jing Qiu. Ultralytics yolol1, 2024. URL <https://github.com/ultralytics/ultralytics>.
- Zaid Khan and Yun Fu. Contrastive alignment of vision to language through parameter-efficient transfer learning. *arXiv preprint arXiv:2303.11866*, 2023.
- Onur Can Koyun, Reyhan Kevser Keser, Ibrahim Batuhan Akkaya, and Behçet Uğur Töreyn. Focus-and-detect: A small object detection framework for aerial images. *Signal Processing: Image Communication*, 104:116675, 2022.
- Weicheng Kuo, Yin Cui, Xiuye Gu, AJ Piergiovanni, and Anelia Angelova. F-vlm: Open-vocabulary object detection upon frozen vision and language models. *arXiv preprint arXiv:2209.15639*, 2022.
- Darius Lam, Richard Kuzma, Kevin McGee, Samuel Dooley, Michael Laielli, Matthew Klaric, Yaroslav Bulatov, and Brendan McCord. xviv: Objects in context in overhead imagery. *arXiv preprint arXiv:1802.07856*, 2018.
- Ke Li, Gang Wan, Gong Cheng, Liqiu Meng, and Junwei Han. Object detection in optical remote sensing images: A survey and a new benchmark. *ISPRS journal of photogrammetry and remote sensing*, 159:296–307, 2020.
- Yan Li, Weiwei Guo, Xue Yang, Ning Liao, Dunnyun He, Jiaqi Zhou, and Wenxian Yu. Toward open vocabulary aerial object detection with clip-activated student-teacher learning. In *European Conference on Computer Vision*, pp. 431–448. Springer, 2024.
- Ye Li, Li Yang, Meifang Yang, Fei Yan, Tonghua Liu, Chensi Guo, and Rufeng Chen. Navblip: a visual-language model for enhancing unmanned aerial vehicles navigation and object detection. *Frontiers in Neurorobotics*, 18:1513354, 2025.
- Tsung-Yi Lin, Michael Maire, Serge Belongie, James Hays, Pietro Perona, Deva Ramanan, Piotr Dollár, and C Lawrence Zitnick. Microsoft coco: Common objects in context. In *Computer vision—ECCV 2014: 13th European conference, zurich, Switzerland, September 6–12, 2014, proceedings, part v 13*, pp. 740–755. Springer, 2014.
- Tsung-Yi Lin, Priya Goyal, Ross Girshick, Kaiming He, and Piotr Dollár. Focal loss for dense object detection. In *Proceedings of the IEEE international conference on computer vision*, pp. 2980–2988, 2017.
- Fan Liu, Delong Chen, Zhangqingyun Guan, Xiaocong Zhou, Jiale Zhu, Qiaolin Ye, Liyong Fu, and Jun Zhou. Remoteclip: A vision language foundation model for remote sensing. *IEEE Transactions on Geoscience and Remote Sensing*, 2024a.
- Shilong Liu, Zhaoyang Zeng, Tianhe Ren, Feng Li, Hao Zhang, Jie Yang, Qing Jiang, Chunyuan Li, Jianwei Yang, Hang Su, et al. Grounding dino: Marrying dino with grounded pre-training for open-set object detection. In *European Conference on Computer Vision*, pp. 38–55. Springer, 2024b.
- Xiaohu Lu, Zuoyue Li, Zhaopeng Cui, Martin R Oswald, Marc Pollefeys, and Rongjun Qin. Geometry-aware satellite-to-ground image synthesis for urban areas. In *Proceedings of the IEEE/CVF Conference on Computer Vision and Pattern Recognition*, pp. 859–867, 2020.
- Xianping Ma, Xiaokang Zhang, Xingchen Ding, Man-On Pun, and Siwei Ma. Decomposition-based unsupervised domain adaptation for remote sensing image semantic segmentation. *IEEE Transactions on Geoscience and Remote Sensing*, 2024.
- Antoine Miech, Jean-Baptiste Alayrac, Lucas Smaira, Ivan Laptev, Josef Sivic, and Andrew Zisserman. End-to-end learning of visual representations from uncurated instructional videos. In *Proceedings of the IEEE/CVF conference on computer vision and pattern recognition*, pp. 9879–9889, 2020.
- Matthias Minderer, Alexey Gritsenko, and Neil Houlsby. Scaling open-vocabulary object detection. *Advances in Neural Information Processing Systems*, 36:72983–73007, 2023.

-
- Emanuele Mule, Matteo Pannacci, Ali Ghasemi Goudarzi, Francesco Pro, Lorenzo Papa, Luca Mariano, and Irene Amerini. Enhancing ground-to-aerial image matching for visual misinformation detection using semantic segmentation. In *Proceedings of the Winter Conference on Applications of Computer Vision*, pp. 795–803, 2025.
- Sahal Shaji Mullappilly, Abhishek Singh Gehlot, Rao Muhammad Anwer, Fahad Shahbaz Khan, and Hisham Cholakkal. Semi-supervised open-world object detection. In *Proceedings of the AAAI Conference on Artificial Intelligence*, volume 38, pp. 4305–4314, 2024.
- Wen Qian, Xue Yang, Silong Peng, Xiujuan Zhang, and Junchi Yan. Rsdet++: Point-based modulated loss for more accurate rotated object detection. *IEEE Transactions on Circuits and Systems for Video Technology*, 32(11):7869–7879, 2022.
- Alec Radford, Jong Wook Kim, Chris Hallacy, Aditya Ramesh, Gabriel Goh, Sandhini Agarwal, Girish Sastry, Amanda Askell, Pamela Mishkin, Jack Clark, et al. Learning transferable visual models from natural language supervision. In *International conference on machine learning*, pp. 8748–8763. PmLR, 2021.
- Kanchana Ranasinghe, Brandon McKinzie, Sachin Ravi, Yinfei Yang, Alexander Toshev, and Jonathon Shlens. Perceptual grouping in contrastive vision-language models. In *Proceedings of the IEEE/CVF International Conference on Computer Vision*, pp. 5571–5584, 2023.
- Joseph Redmon, Santosh Divvala, Ross Girshick, and Ali Farhadi. You only look once: Unified, real-time object detection. In *Proceedings of the IEEE conference on computer vision and pattern recognition*, pp. 779–788, 2016.
- Krishna Regmi and Mubarak Shah. Bridging the domain gap for ground-to-aerial image matching. In *Proceedings of the IEEE/CVF International Conference on Computer Vision*, pp. 470–479, 2019.
- Shaoqing Ren, Kaiming He, Ross Girshick, and Jian Sun. Faster r-cnn: Towards real-time object detection with region proposal networks. *Advances in neural information processing systems*, 28, 2015.
- Linus Scheibenreif, Michael Mommert, and Damian Borth. Parameter efficient self-supervised geospatial domain adaptation. In *Proceedings of the IEEE/CVF Conference on Computer Vision and Pattern Recognition*, pp. 27841–27851, 2024.
- Qi Shan, Changchang Wu, Brian Curless, Yasutaka Furukawa, Carlos Hernandez, and Steven M Seitz. Accurate geo-registration by ground-to-aerial image matching. In *2014 2nd International Conference on 3D Vision*, volume 1, pp. 525–532. IEEE, 2014.
- Maxim Shugayev, Ilya Semenov, Kyle Ashley, Michael Klaczynski, Naresh Cuntoor, Mun Wai Lee, and Nathan Jacobs. Arcgeo: Localizing limited field-of-view images using cross-view matching. In *Proceedings of the IEEE/CVF Winter Conference on Applications of Computer Vision*, pp. 209–218, 2024.
- PJ Soto, GAOP Costa, RQ Feitosa, PN Happ, MX Ortega, J Noa, CA Almeida, and Christian Heipke. Domain adaptation with cyclegan for change detection in the amazon forest. *ISPRS Archives*; 43, B3, 43(B3):1635–1643, 2020.
- Bin Wang, Fei Deng, Shuang Wang, Wen Luo, Zhixuan Zhang, Gulan Zhang, and Peifan Jiang. Siamseg: Self-training with contrastive learning for unsupervised domain adaptation semantic segmentation in remote sensing. *arXiv preprint arXiv:2410.13471*, 2024a.
- Kun Wang, Zi Wang, Zhang Li, Xichao Teng, and Yang Li. Multi-scale cross distillation for object detection in aerial images. In *European Conference on Computer Vision*, pp. 452–471. Springer, 2024b.
- Maciej K Wozniak, Mattias Hansson, Marko Thiel, and Patric Jensfelt. Uada3d: Unsupervised adversarial domain adaptation for 3d object detection with sparse lidar and large domain gaps. *IEEE Robotics and Automation Letters*, 2024.

-
- Fan Yang, Heng Fan, Peng Chu, Erik Blasch, and Haibin Ling. Clustered object detection in aerial images. In *Proceedings of the IEEE/CVF international conference on computer vision*, pp. 8311–8320, 2019a.
- Xue Yang, Jirui Yang, Junchi Yan, Yue Zhang, Tengfei Zhang, Zhi Guo, Xian Sun, and Kun Fu. Scrdet: Towards more robust detection for small, cluttered and rotated objects. In *Proceedings of the IEEE/CVF international conference on computer vision*, pp. 8232–8241, 2019b.
- Xue Yang, Junchi Yan, Ziming Feng, and Tao He. R3det: Refined single-stage detector with feature refinement for rotating object. In *Proceedings of the AAAI conference on artificial intelligence*, volume 35, pp. 3163–3171, 2021.
- Liang Yao, Fan Liu, Chuanyi Zhang, Zhiquan Ou, and Ting Wu. Domain-invariant progressive knowledge distillation for uav-based object detection. *IEEE Geoscience and Remote Sensing Letters*, 2024.
- Junyan Ye, Jun He, Weijia Li, Zhutao Lv, Jinhua Yu, Haote Yang, and Conghui He. Skydiffusion: Street-to-satellite image synthesis with diffusion models and bev paradigm. *arXiv preprint arXiv:2408.01812*, 2024.
- Alireza Zareian, Kevin Dela Rosa, Derek Hao Hu, and Shih-Fu Chang. Open-vocabulary object detection using captions. In *Proceedings of the IEEE/CVF conference on computer vision and pattern recognition*, pp. 14393–14402, 2021.
- Junying Zeng, Yajin Gu, Chuanbo Qin, Xudong Jia, Senyao Deng, Jiahua Xu, and Huiming Tian. Unsupervised domain adaptation for remote sensing semantic segmentation with the 2d discrete wavelet transform. *Scientific Reports*, 14(1):23552, 2024.
- Huiying Zhang, Pan Xiao, Feifan Yao, Qinghua Zhang, and Yifei Gong. Fusion of multi-scale attention for aerial images small-target detection model based on pare-yolo. *Scientific Reports*, 15(1):4753, 2025.
- Yuanlin Zhang, Yuan Yuan, Yachuang Feng, and Xiaoqiang Lu. Hierarchical and robust convolutional neural network for very high-resolution remote sensing object detection. *IEEE Transactions on Geoscience and Remote Sensing*, 57(8):5535–5548, 2019.
- Yiwu Zhong, Jianwei Yang, Pengchuan Zhang, Chunyuan Li, Noel Codella, Liunian Harold Li, Luowei Zhou, Xiyang Dai, Lu Yuan, Yin Li, et al. Regionclip: Region-based language-image pretraining. In *Proceedings of the IEEE/CVF conference on computer vision and pattern recognition*, pp. 16793–16803, 2022.
- Xingyi Zhou, Rohit Girdhar, Armand Joulin, Philipp Krähenbühl, and Ishan Misra. Detecting twenty-thousand classes using image-level supervision. In *European conference on computer vision*, pp. 350–368. Springer, 2022.
- Xizhou Zhu, Weijie Su, Lewei Lu, Bin Li, Xiaogang Wang, and Jifeng Dai. Deformable detr: Deformable transformers for end-to-end object detection. *arXiv preprint arXiv:2010.04159*, 2020.

A APPENDIX

A.1 MODEL-AGNOSTIC CONTRASTIVE ALIGNMENT STRATEGY

Experimental results on the VisDrone dataset demonstrate the model-agnostic nature of our framework, as shown using OWLv2 and GroundingDINO. Given any open-vocabulary ground-view detector, we generate cross-view data which, combined with our contrastive alignment strategy, enables the construction of an open-vocabulary aerial-view detector—without being tied to a specific architecture like OWLv2. As seen in 7, the framework transfers seamlessly across models and facilitates effective ground-to-aerial adaptation.

Model	Finetuned	Ours <i>mAP</i>
OWLv2 Minderer et al. (2023)	25.70	44.97 (+19.27)
GroundingDINO Liu et al. (2024b)	33.00	47.15 (+14.15)

Table 7: Model-agnostic results on the VisDrone dataset.

A.2 QUALITATIVE RESULTS



Figure 8: Qualitative results on xView Lam et al. (2018)



Figure 9: Qualitative results on DOTAv2 Ding et al. (2021)



Figure 10: Qualitative results on VisDrone Cao et al. (2021)